# Optimal Renewable Resources Mix for Distribution System Energy Loss Minimization

Y. M. Atwa, *Student Member, IEEE*, E. F. El-Saadany, *Senior Member, IEEE*, M. M. A. Salama, *Fellow, IEEE*, and R. Seethapathy, *Member, IEEE*

***Abstract*—It is widely accepted that renewable energy sources are the key to a sustainable energy supply infrastructure since they are both inexhaustible and nonpolluting. A number of renewable energy technologies are now commercially available, the most notable being wind power, photovoltaic, solar thermal systems, biomass, and various forms of hydraulic power. In this paper, a methodology has been proposed for optimally allocating different types of renewable distributed generation (DG) units in the distribution system so as to minimize annual energy loss. The methodology is based on generating a probabilistic generation-load model that combines all possible operating conditions of the renewable DG units with their probabilities, hence accommodating this model in a deterministic planning problem. The planning problem is formulated as mixed integer nonlinear programming (MINLP), with an objective function for minimizing the system's annual energy losses. The constraints include the voltage limits, the feeders' capacity, the maximum penetration limit, and the discrete size of the available DG units. This proposed technique has been applied to a typical rural distribution system with different scenarios, including all possible combinations of the renewable DG units. The results show that a significant reduction in annual energy losses is achieved for all the proposed scenarios.**

***Index Terms*—Distributed generation, distribution system planning, fuel mix, uncertainty.**

## I. Introduction

ELECTRICAL power systems are evolving from today's centralized bulk systems, with generation plants connected to the transmission network, to more decentralized systems, with smaller generating units connected directly to distribution networks close to demand consumption. This type of generating unit is known as distributed generation (DG). Environmental consciousness and sustainable development based on long-term diversification of energy sources are key drivers of these changes, which have contributed to the promotion of renewable energy sources.

Technologies that can supply renewable power to consumers at reasonable prices without degrading the security and reliability of the distribution system have vast potential. If this goal of effectively incorporating renewable power into the electricity supply is to be achieved, the special technical and economic challenges that the intermittent nature of renewable power generation introduces must be met.

Manuscript received March 05, 2009; revised April 14, 2009. First published October 30, 2009; current version published January 20, 2010. Paper no. TPWRS-00083-2009.

Y. M. Atwa, E. F. El-Saadany, and M. M. A. Salama are with the Department of Electrical and Computer Engineering, University of Waterloo, Waterloo, ON N2L 3G1, Canada (e-mail: ymoustaf@uwaterloo.ca).

R. Seethapathy is with Hydro One Network, Inc., Toronto, ON M5G 2P5, Canada.

Color versions of one or more of the figures in this paper are available online at http://ieeexplore.ieee.org.

Digital Object Identifier 10.1109/TPWRS.2009.2030276

Proper allocation of DG units into an existing distribution system plays a crucial role in the improvement of the system's performance; therefore, optimal allocation of DG is one of the most important aspects of DG planning. Considering total power penetration from DG units, [1] and [2] employed the Hereford Ranch algorithm to minimize system losses. With the same objective, [3] presented an iterative technique to determine the near optimal placement of DG units on the power grid. The studies in [5] and [6] utilized an iterative methodology for the allocation of DG units in the distribution system. They used an analysis of power flow equations for both voltage sensitivity and loss sensitivity in order to identify the best sites for placing DG units in the distribution system. In [7], an iterative optimal power flow-based technique was proposed to allocate new generation capacity on predetermined connection points within the existing network. The work considered the network constraints including the fault level constraints imposed by switchgear capabilities. In [8], the optimal penetrations of different DG technologies were determined by analyzing the effect that changing the penetration level had on annual energy losses. A heuristic approach to DG-capacity investment planning with respect to competitive electricity market auctions was proposed in [9]. The optimal allocations of DG units were obtained through a cost-benefit analysis from the perspective of a distribution company. The work in [10] proposed a multi-objective formulation for sizing DG resources and fitting them into existing distribution networks. The methodology permits the planner to decide on the best compromise between the cost of network upgrading, the cost of power losses, the cost of energy not supplied, and the cost of the energy required by the customers served. In [11], an analytical technique was proposed for optimally allocating DG units in a radial distribution system that minimizes power losses. The proposed technique considered different types of load profiles with varying time loads and DG output while also taking into account technical constraints, such as feeder capacity limits and voltage profile. In [12], a GA algorithm was applied for the optimal allocation of DG units in a distribution system. To handle the effect of the uncertainties associated with DG penetration and protection, [13] and [14] used a heuristic optimization algorithm based on decision theory. The work in [15] proposed a multiperiod steady-state analysis for maximizing the connection of intermittent distributed generation through an optimal power flow-based technique. The proposed technique considered the different loading levels of the system under study, as well as

0885-8950/$26.00 © 2009 IEEE

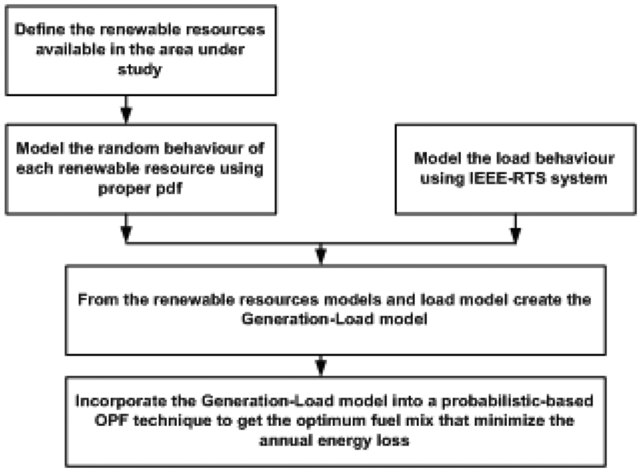


Fig. 1. Block diagram of the proposed work.

the intermittent nature of wind outputs. For determining the optimal fuel mix of different DG technologies, [16] and [17] formulated a mixed integer linear program to optimally utilize the available energy resources for a section of a distribution network. The objective function incorporates loss adjustment factors (LAFs) along with individual generation load factors (LFs), thus facilitating the determination of the optimal DG plant mix for a network section.

This review of the literature shows that considerable work has been done with respect to the allocation of DG units in the distribution system; however, most of the work presented assumes that the output of the DG is dispatchable and controllable. Most of the available methods are unable to model the intermittent nature of the output power. To the authors' knowledge, only a few studies have considered the uncertainties in the power output from renewable DG units [11], [13]–[15] or the optimal fuel mix problem [16], [17]. Hence, the problem regarding the optimal allocation and fuel mix of renewable DG units still requires attention.

In this work, as in Fig. 1, a probabilistic-based planning technique is proposed for determining the optimal fuel mix of different types of renewable DG units (i.e., wind-based DG, solar DG, and biomass DG) in order to minimize the annual energy losses in the distribution system without violating the system constraints. The proposed algorithm takes into consideration both the discrete size and maximum allowable penetration limits of the DG. The problem is formulated as mixed integer nonlinear programming (MINLP), taking into consideration the uncertainty associated with the renewable DG resources as well as the hourly variations in the load profile.

The paper is organized as follows: the next six sections explain the objective function, the renewable resource modeling, the load modeling, and the combined generation-load modeling. Section VIII presents the mathematical formulation of the proposed planning technique, and Section IX introduces a sample case study of a distribution system. The results and conclusions are presented in Sections X and XI, respectively.

## II. Objective Function

Due to the environmental concerns and fuel cost uncertainties associated with the use of conventional energy sources, attention has been directed toward implementing renewable DG units in distribution systems. Therefore, in Canada, based on Ontario's Standard Offer Program (SOP) [18], local distribution companies (LDCs) are required to accept a given percentage of *customer-owned* wind-based DG units in their system. Consequently, LDCs can use the proposed method to select the allocations that will maximize benefits.

In general, benefit maximization in any normal planning problem means minimizing cost while maintaining the performance of the system within acceptable limits. Costs include the following.

- *Capital cost*: In this case, the capital cost of the renewable DG units is the sole responsibility of the customer.
- *Running cost (operation and maintenance cost)*: As with the capital cost, operation and maintenance are the sole responsibilities of the customer.
- *Cost of unserved energy due to interruption (maximizing the system reliability)*: Based on the current practice of deploying DG units in distribution systems, this cost represents the impact of renewable DG on the reliability of such distribution systems. In this regard, the following should be noted.
  1) A distribution network is fed from a transmission network, and when the connection to the transmission system is lost, i.e., the distribution network is islanded, all DG units are required to shut down for loss-of-main protection. This practice is normal, and DG therefore does not play a role in increasing the reliability of the supply [19].
  2) If islanding is allowed, the system cannot rely solely on renewable DG units to supply the island's load. Renewable DG units are characterized by high levels of random power fluctuation that result in power mismatch issues, causing stability problems with respect to voltage and frequency [20].
  3) Conversely, renewable DG has the potential to increase the reliability of the system from the perspective of relieving substation transformers and main feeders during peak load periods. This relief may result in extending the usable lifetime of the transformer and reducing the probability of premature failure due to overloading. However, this potential increase in reliability does not depend on the placement of the DG units on the feeders and is therefore outside the scope of this study. Thus, for the purposes of this study, it is assumed that the location of renewable DG units on a given feeder has no direct influence on the reliability of the distribution system.
- *Feeder power losses*: Network losses are a key consideration in the planning problem for the following reasons.
  1) While DG may unload lines and reduce losses, if they are improperly allocated, the reverse power flows from larger DG units can give rise to excessive losses and can overheat feeders.
  2) Minimizing system power losses has a positive impact on relieving the feeders, reducing the voltage drop, and improving the voltage profile and has other environmental and economical benefits.

Therefore, based on these considerations, the objective of the proposed planning problem is, for all possible operating conditions, to minimize the annual energy losses of the system without violating system constraints.

## III. Modeling of Renewable Resources and Load Data

This section explains the generation of the proposed models of both renewable resources and load. A selected study period of one year is divided into four seasons, and a typical day is generated for each season in order to represent the random behavior of the different renewable resources during each period. For the site under study, the hourly solar irradiance and wind speed data are modeled by Beta and Weibull probability density functions (pdf), respectively. The biomass is considered to be a firm generation, and the IEEE-RTS system is utilized to generate the load model.

### A. Historical Data Processing

The Beta and Weibull probability distribution functions that are required for estimating the hourly solar irradiance and wind speed are based on three years of historical data that have been collected from the site under study. Each year is divided into four seasons, with each season being represented by any day within that season. The data are then utilized to generate for each season a typical day's frequency distribution of the irradiance and wind speed measurements. The day representing each season is further subdivided into 24-h segments (time segments), each referring to a particular hourly interval for the entire season. Thus, there are 96 time segments for the year (24 for each season). Considering a month to be 30 days, each time segment then has 270 irradiance and wind speed level data points $(3\ \text{years} \times 30\ \text{days per month} \times 3\ \text{months per season})$. From these data, the mean and standard deviation for each time segment are calculated, and from them, the Beta and Weibull probability density functions are generated for each hour, as described below.

### B. Solar Irradiance Modeling

For the same hour of the typical day in each season, the irradiance data usually have a bimodal distribution function. The data are divided into two groups, each group having a unimodal distribution function. Therefore, to describe the random phenomenon of the irradiance data, a Beta pdf is utilized for each unimodal [21], as set out in the following:

$$f_b(s) = \begin{cases} \frac{\Gamma(\alpha+\beta)}{\Gamma(\alpha)\Gamma(\beta)} * s^{(\alpha-1)} & \\ \quad *(1-s)^{(\beta-1)}, & \text{for } 0 \le s \le 1, \alpha \ge 0, \beta \ge 0 \\ 0, & \text{otherwise} \end{cases} \tag{1}$$

where

$s$ solar irradiance $\mathrm{kW/m^2}$;

$f_b(s)$ Beta distribution function of $s$;

$\alpha, \beta$ parameters of the Beta distribution function.

To calculate the parameters of the Beta distribution function, the mean $(\mu)$ and standard deviation $(\sigma)$ of the random variable $s$ are utilized as follows:

$$\beta = (1-\mu) * \left( \frac{\mu * (1+\mu)}{\sigma^2} - 1 \right) \tag{2}$$

$$\alpha = \frac{\mu * \beta}{1-\mu}. \tag{3}$$

### C. Wind Speed Modeling

A very good expression often recommended for modeling the behavior of wind speed is the Weibull pdf $(f_w(v))$ (4). This recommendation is based on a comparison of actual wind speed profiles at different sites and wind speed profiles estimated using the Weibull pdf [22], especially for $k = 2$:

$$f_w(v) = \frac{k}{c}\left(\frac{v}{c}\right)^{k-1} \exp\left[-\left(\frac{v}{c}\right)^k\right] \tag{4}$$

where $k$ is called the shape index, and $c$ is called the scale index. When the shape index $k$ equals 2, the pdf is called a Rayleigh pdf $(f_r(v))$ as given in (5). This pdf mimics most wind speed profiles; therefore, it is used in this study to model the wind speed for each time segment:

$$f_r(v) = \left(\frac{2v}{c^2}\right) \exp\left[-\left(\frac{v}{c}\right)^2\right]. \tag{5}$$

The Rayleigh scale index $c$ can be found using the following acceptable approximation:

$$c \approx 1.128 v_m. \tag{6}$$

### D. Biomass Modeling

The biomass DG is considered as a firm generation DG. In other words, the output power of such DG is considered constant at its rated value with no associated uncertainties.

### E. Load Modeling

The load profile is assumed to follow the IEEE-RTS [23] system. This system provides hourly peak load as a percentage of the daily peak load.

## IV. State Selection

To incorporate the output power of the solar DG and wind-based DG units as multistate variables in the planning formulation, the continuous pdf of each has been divided into states (periods), in each of which the solar irradiance and wind speed are within specific limits. In other words, for each time segment, there are a number of states for the solar irradiance and wind speed. The number of states is carefully selected for the Beta and Rayleigh distributions because a small number of states affects accuracy, while a large number increases the complexity of the problem. In this work, the step is adjusted to be $0.1\ \mathrm{Kw/m^2}$ for the solar irradiance and 1 m/s for wind speed.

The probability of the solar irradiance and wind speed DG for each state during any specific hour is calculated using (7) and (8), respectively:

$$P_s\{G_y\} = \int_{s_{y1}}^{s_{y2}} f_b(v).dv \tag{7}$$

$$P_v\{G_w\} = \int_{v_{w1}}^{v_{w2}} f_r(v).dv \tag{8}$$

where

| | |
|---|---|
| $P_s\{G_y\}$ | probability of the solar irradiance being in state $y$; |
| $P_v\{G_w\}$ | probability of wind speed being in state $w$; |
| $s_{y1}$ and $s_{y2}$ | solar irradiance limits of state $y$; |
| $v_{w1}$ and $v_{w2}$ | wind speed limits of state $w$. |

## V. Calculation of the Output of the PV Module and Wind Turbine Power

This section describes the calculation of the output power of the PV module and the wind turbine corresponding to each state, using the characteristics of the PV module and the wind turbine power performance curve. For simplicity, the average value of each state is utilized to calculate the output power for that state [e.g., for wind speed, if the second state has limits of 1 m/s and 2 m/s, the average value for this state is $(v_{a2}) = 1.5\ \mathrm{m/s}$].

### A. Calculation of the PV Module Output Power

The output power of the PV module is dependent on the solar irradiance and ambient temperature of the site as well as the characteristics of the module itself. Therefore, once the Beta pdf is generated for a specific time segment, the output power during the different states is calculated for this segment using the following:

$$Tc_y = T_A + s_{ay}\left(\frac{N_{OT} - 20}{0.8}\right) \tag{9}$$

$$Iy = s_{ay}\left[I_{sc} + K_i(Tc - 25)\right] \tag{10}$$

$$V_y = V_{oc} - K_v * Tc_y \tag{11}$$

$$P_{Sy}(s_{ay}) = N * FF * V_y * I_y \tag{12}$$

$$FF = \frac{V_{MPP} * I_{MPP}}{V_{oc} * I_{sc}} \tag{13}$$

where

| | |
|---|---|
| $T_{cy}$ | cell temperature $^\circ\mathrm{C}$ during state $y$; |
| $T_A$ | ambient temperature $^\circ\mathrm{C}$; |
| $K_v$ | voltage temperature coefficient $\mathrm{V}/^\circ\mathrm{C}$; |
| $K_i$ | current temperature coefficient $\mathrm{A}/^\circ\mathrm{C}$; |
| $N_{OT}$ | nominal operating temperature of cell in $^\circ\mathrm{C}$; |
| $FF$ | fill factor; |
| $I_{sc}$ | short circuit current in A; |
| $V_{oc}$ | open-circuit voltage in V; |
| $I_{MPP}$ | current at maximum power point in A; |
| $V_{MPP}$ | voltage at maximum power point in V; |
| $P_{Sy}$ | output power of the PV module during state $y$; |
| $s_{ay}$ | average solar irradiance of state $y$. |

### B. Calculation of the Output Power of a Wind Turbine

The output power of a wind turbine is dependent on the wind speed at the site as well as the parameters of the power performance curve. Therefore, once the Rayleigh pdf is generated for a specific time segment, the output power during the different states is calculated for this segment using the following equation [24]:

$$P_{Vw}(v_{aw}) = \begin{cases} 0 & 0 \le v_{aw} \le v_{ci} \\ P_{rated} * \frac{(v_{aw} - v_{ci})}{(v_{aw} - v_{ci})} & v_{ci} \le v_{aw} \le v_r \\ P_{rated} & v_r \le v_{aw} \le v_{co} \\ 0 & v_{co} \le v_{aw} \end{cases} \tag{14}$$

where

| | |
|---|---|
| $v_{ci}$, $v_r$ and $v_{co}$ | cut in speed, rated speed, and cut-off speed of the wind turbine, respectively; |
| $P_{Vw}$ | output power of the wind turbine during state $w$; |
| $v_{aw}$ | average wind speed of state $w$. |

## VI. Site Matching

This section details the steps for selecting the optimum PV module and wind turbine for a specific site. The selection is based on the capacity factor (CF) of the available PV modules and wind turbines. A capacity factor can be defined as the ratio between the average output power and the rated power. The hourly average output power of a PV module or a wind turbine is the summation of the power produced at all possible states for this hour multiplied by the corresponding probability of each state. Once the average output power is calculated for each time segment, the average output power is calculated for the typical day in each season, and hence, the annual average output power.

For this study, the optimal PV module or wind turbine is selected based on the highest CF criteria. However, it must be mentioned that selecting the candidate wind turbine based on the highest CF may not lead to optimal loss minimization from a planning perspective because implementing the highest CF restricts the search area to a multiple of the selected wind turbine rating (e.g., if the turbine with the highest CF has a rating of 1 MW, then the wind-based DG penetration at the candidate buses must be a multiple of that rating).

This problem does not appear with PV modules because their ratings are very small compared to the required amount of solar DG (e.g., if the PV module with the highest CF has a rating of 60 W and the required solar DG penetration is 1.236 MW at a specific bus, this level can be achieved by using a PV panel consisting of 20 600 modules).

## VII. Combined Generation-Load Model

The modeling of different types of renewable DG and the load are utilized to generate a combined annual generation-load model. Assuming that wind speed states and solar irradiance states are independent, the probability of any combination of them $(P\{C_g\})$ is obtained by convolving the two probabilities, as given in the following:

$$P\{C_g\} = P_v\{G_w\} * P_s\{G_y\}. \tag{15}$$

Since the load and the output power of the biomass DG units are constant during each hour, the probability of each is 1. Hence, they are not incorporated into (15).

Based on this concept, a generation-load model for different types of renewable DG units is obtained by listing all possible combinations of renewable DG output power and the load for the whole year. The complete generation-load model is given as follows:

$$R = [\{C_g, P\{C_g\}\} : g = 1 : N] \tag{16}$$

where

- $R$ complete annual generation-load model;
- $C$ matrix of four columns that include all possible combinations of the wind output power states and solar output power states as well as the load states and the firm generation of the biomass DG (i.e., column 1 represents the output power of wind-based DG as a percentage of the rated power, column 2 represents the output power of the solar DG as a percentage of the rated power, column 3 represents the constant output power of the biomass DG, and column 4 represents the different load levels);
- $P\{C_g\}$ one-column matrix that represents the probability corresponding to matrix $C$;
- $N$ total number of discrete states in model $R$, which is equal to the product of the wind speed states and the solar irradiance states.

A small-scale example of the generation-load model is presented in the Appendix.

## VIII. Planning Problem Formulation

This section presents the proposed probabilistic formulation for a local distribution company's (LDC) planning problem with respect to the system under study. The rationale behind the proposed technique is to accommodate the probabilistic generation-load model into the deterministic optimal power flow (OPF) equations. In other words, the number of active/reactive power flow equations, (18) and (19), is equal to the total number of states. For each state, the penetration of the renewable DG units is changed based on the generation-load model, while the power loss is calculated and then weighted according to the probability of occurrence of this state during the entire year, in order to calculate the energy losses. The optimum allocations of the DG units are then determined so that, for all operating conditions, the total energy losses are minimized without violating the system constraints.

To formulate an accurate planning strategy that determines the optimal fuel mix of renewable DG units, the following assumptions are made.

- More than one type of DG can be connected to the same bus.
- All the DG units are working at a unity power factor.
- The LDC will not make any upgrades in the system as a consequence of connecting the DG units, such as changing the feeders or adding regulating stations.
- In the radial system under study, there is an assumed maximum limit for investing in DG capacities for each bus [9].
- For the sake of simplicity, it is assumed that all buses in the system under study are subjected to the same wind profile and solar irradiance; if it is not true, it only complicates the generation-load model.

For determining the optimal fuel mix of renewable resources, seven scenarios are proposed, along with an extra reference scenario for comparison:

*Scenario #1*: the reference scenario, in which no DG units are connected to the system (base case);
*Scenario #2*: only wind-based DG;
*Scenario #3*: only biomass DG units;
*Scenario #4*: only solar DG units;
*Scenario #5*: wind-based DG with solar DG;
*Scenario #6*: wind-based DG with biomass DG;
*Scenario #7*: solar DG with biomass DG.
*Scenario#8*: a mix of wind-based, solar and biomass DG.

The mathematical formulation is described in (17)–(28). This model is formulated as MINLP on a GAMS environment [25]. Since most of the distribution systems have a radial topology, in the formulation, bus 1 is the substation bus.

### A. Objective Function

The objective of the planning formulation is to minimize the annual energy losses in the distribution system for all possible combinations of load and DG output power. Since each time segment represents 90 h (30 days per month × 3 months per season), the objective function can be described as follows:

$$\text{Minimize} \quad Cost = \sum_{g=1}^{N} P_{loss_g} * P\{C_g\} * 90 \tag{17}$$

where $P_{loss_g}$ is the total power losses in the system during state $g$.

### B. Constraints

*1) Power Flow Equations:*

$$\begin{aligned} &P_{G_{g,1}} + C(g,1)*P_{DGW_i} + C(g,2)*P_{DGS_i} \\ &\quad + C(g,3)*P_{DGb_i} - C(g,4)*P_{D_i} \\ &\quad = \sum_{j=1}^{n} V_{g,i}*V_{g,i}*Y_{ij}*\cos(\theta_{ij}+\delta_{g,j}-\delta_{g,i}), \quad \forall i,g \end{aligned} \tag{18}$$

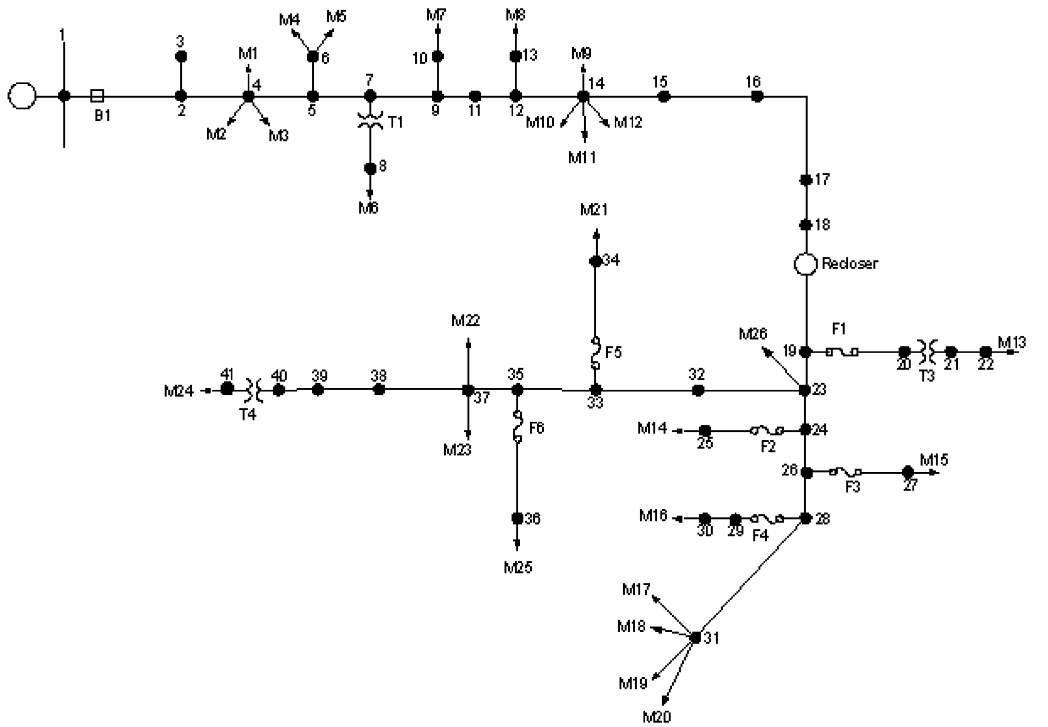


Fig. 2. System under study.

$$Q_{G_{g,1}} - C(g,4) * Q_{D_{g,i}} = -\sum_{j=1}^{n} V_{g,i} * V_{g,i} * Y_{ij} * \sin(\theta_{ij} + \delta_{g,j} - \delta_{g,i}), \quad \forall i, g \quad (19)$$

where

| | |
|---|---|
| $P_{DGWi}$ | rated power of the wind-based DG connected at bus $i$; |
| $P_{DGSi}$ | rated power of the solar DG connected at bus $i$; |
| $P_{DGbi}$ | rated power of the biomass DG connected at bus $i$; |
| $P_{G1}$ | substation active power injected; |
| $Q_{G1}$ | substation reactive power injected; |
| $P_{Di}$ | peak active load at bus $i$; |
| $Q_{Di}$ | peak reactive load at bus $i$; |
| $V_{g,i}$ | voltage at bus i during state $g$; |
| $n$ | total number of buses in the system. |

*2) Power Loss Equations:*

$$P_{loss_g} = 0.5 * \sum_{i=1}^{n} \sum_{j=1}^{n} G_{ij} * \left[ (V_{g,i})^2 + (V_{g,j})^2 - 2 * V_{g,i} * V_{g,j} * \cos(\delta_{g,j} - \delta_{g,i}) \right], \quad \forall g. \quad (20)$$

*3) Branch Current Equations:*

$$I_{g,ij} = |Y_{ij}| * \left[ (V_{g,i})^2 + (V_{g,j})^2 - 2 * V_{g,i} * V_{g,j} * \cos(\delta_{g,j} - \delta_{g,i}) \right]^{1/2}, \quad \forall g, i, j \quad (21)$$

where $I_{g,i,j}$ is the current in the feeder connecting busses $i$ and $j$ during state $g$.

*4) Slack Bus Voltage and Angle (Assumed to be Bus 1):*

$$V_{g,1} = 1.0 \qquad \delta_{g,1} = 0.0. \quad (22)$$

*5) Voltage Limits at the Other Buses:*

$$V_{\min} \leq V_{g,i} \leq V_{\max}, \forall i \notin substation\ bus,\ g. \quad (23)$$

*6) Feeder Capacity Limits:*

$$0 \leq I_{g,ij} \leq I_{ij_{\max}}, \qquad \forall i, j, g. \quad (24)$$

*7) Discrete Size of the DG Units:*

*a) Wind-based DG units:*

$$P_{DGW_i} = a_{w1,i}.P_{rw1} + a_{w2,i}.P_{rw2} + \ldots \quad \forall i \in B \quad (25)$$

where

| | |
|---|---|
| $a_{w1,i}, a_{w2,i} \ldots$ | integer variables; |
| $Prw_1, Prw_2 \ldots$ | available ratings of the wind-based DG units; |
| $B$ | set of candidate buses to connect DG units. |

*b) Biomass DG units:*

$$P_{DGb_i} = a_{b1,i}.P_{rb1} + a_{b2,i}.P_{rb2} + \ldots \quad \forall i \in B \quad (26)$$

TABLE I
CHARACTERISTICS OF THE WIND TURBINES AVAILABLE

| Features | Turbine 1 | Turbine 2 | Turbine 3 | Turbine 4 |
|---|---|---|---|---|
| Rated power | 850 KW | 1.1 MW | 2 MW | 3 MW |
| Cut-in speed (m/s) | 4 | 4 | 4 | 4 |
| Rated speed (m/s) | 16 | 14 | 15 | 15 |
| Cut-out speed (m/s) | 25 | 24 | 25 | 25 |

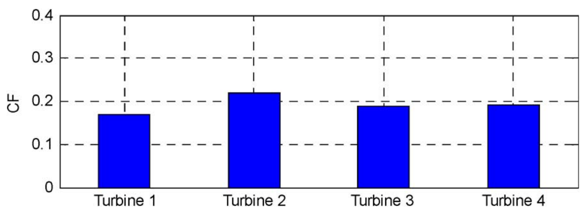


Fig. 3. CF of the wind turbines available.

where

$a_{b1,i}, a_{b2,i} \cdots$ integer variables;

$Prb_1, Prb_2 \ldots$ available ratings of the biomass DG units.

*c) Solar DG units:* Unlike the wind-based DG and the biomass DG, the solar DG rating has no limit because the PV array can be arranged to generate almost the power required.

*8) Maximum Penetration on Each Bus:*

$$P_{DGW_i} + P_{DGS_i} + P_{DGb_i} \leq P_{bus}, \quad \forall i \in B \tag{27}$$

where $P_{bus}$ is the maximum penetration allowable on each bus.

*9) Maximum Penetration of DG Units in the System:* The maximum penetration limit is calculated based on the average penetration of the renewable DG units:

$$\sum_{i=1}^{n} CF_w * P_{DGW_i} + \sum_{i=1}^{n} CF_s * P_{DGS_i} + \sum_{i=1}^{n} P_{DGb_i} \leq x * \sum_{i=1}^{n} P_{D_i} \tag{28}$$

where $x$ is the maximum penetration limit as a percentage of the peak load.

## IX. CASE STUDY

This section presents the general data, wind speed data, and wind turbine data for the system under study.

### A. System Under Study

The system under study, as shown in Fig. 2, is a typical rural distribution system with a peak load of 16.18 MVA. The main substation at bus 1 is used to feed a rural area, and the maximum feeder capacity is 300 A.

For this study, the candidate buses for connecting the DG units are included in the set $B : \{19, 23, 24, 26, 28, 32, 33, 35, 37, 38, 39, 40\}$, based on Ontario's standard offer program [18], the maximum limit for investing in DG capacities on each bus is 10 MW (i.e., $P_{bus} = 10$ MW), and the maximum penetration limit is 30% of the peak load (i.e., $x = 0.3$).

TABLE II
CHARACTERISTICS OF THE PV MODULES AVAILABLE

| Module characteristics | Module type | | | |
|---|---|---|---|---|
| | A | B | C | D |
| Watt peak (W) | 50.00 | 53.00 | 60.00 | 75.00 |
| Open circuit voltage (V) | 55.50 | 21.70 | 21.10 | 21.98 |
| Short circuit current (A) | 1.80 | 3.40 | 3.80 | 5.32 |
| Voltage at maximum power (V) | 38.00 | 17.40 | 17.10 | 17.32 |
| Current at maximum power (A) | 1.32 | 3.05 | 3.50 | 4.76 |
| Voltage temperature coefficient (mV/°C) | 194.00 | 88.00 | 75.00 | 14.40 |
| Current temperature coefficient (mA/°C) | 1.40 | 1.50 | 3.10 | 1.22 |
| Nominal cell operating temperature (°C) | 43.00 | 43.00 | 43.00 | 43.00 |

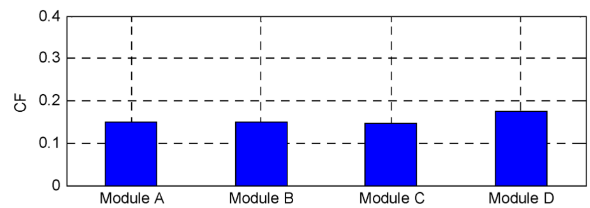


Fig. 4. CF of the PV modules available.

TABLE III
LOAD DATA FOR THE SYSTEM UNDER STUDY

| Hour | Winter | Spring | Summer | Fall |
|---|---|---|---|---|
| 12-1 am | 0.4757 | 0.3969 | 0.64 | 0.3717 |
| 1--2 | 0.4473 | 0.3906 | 0.60 | 0.3658 |
| 2--3 | 0.4260 | 0.3780 | 0.58 | 0.3540 |
| 3--4 | 0.4189 | 0.3654 | 0.56 | 0.3422 |
| 4--5 | 0.4189 | 0.3717 | 0.56 | 0.3481 |
| 5--6 | 0.4260 | 0.4095 | 0.58 | 0.3835 |
| 6--7 | 0.5254 | 0.4536 | 0.64 | 0.4248 |
| 7--8 | 0.6106 | 0.5355 | 0.76 | 0.5015 |
| 8--9 | 0.6745 | 0.5985 | 0.87 | 0.5605 |
| 9--10 | 0.6816 | 0.6237 | 0.95 | 0.5841 |
| 10--11 | 0.6816 | 0.6300 | 0.99 | 0.5900 |
| 11--12pm | 0.6745 | 0.6237 | 1.00 | 0.5841 |
| 12--1 | 0.6745 | 0.5859 | 0.99 | 0.5487 |
| 1--2 | 0.6745 | 0.5796 | 1.00 | 0.5428 |
| 2--3 | 0.6603 | 0.5670 | 1.00 | 0.5310 |
| 3--4 | 0.6674 | 0.5544 | 0.97 | 0.5192 |
| 4--5 | 0.7029 | 0.5670 | 0.96 | 0.5310 |
| 5--6 | 0.7100 | 0.5796 | 0.96 | 0.5428 |
| 6--7 | 0.7100 | 0.6048 | 0.93 | 0.5664 |
| 7--8 | 0.6816 | 0.6174 | 0.92 | 0.5782 |
| 8--9 | 0.6461 | 0.6048 | 0.92 | 0.5664 |
| 9--10 | 0.5893 | 0.5670 | 0.93 | 0.5310 |
| 10--11 | 0.5183 | 0.5040 | 0.87 | 0.4720 |
| 11--12am | 0.4473 | 0.4410 | 0.72 | 0.4130 |

### B. Wind Speed and Wind Turbine Data

The hourly wind speed data for the site under study have been utilized to generate a Rayleigh pdf for each time segment and thus to calculate the CF for each available wind turbine, as listed

TABLE IV
RESULTS USING DISCRETE DG SIZES

| Candidate Buses | No DG | Wind | Biomass | Solar | Wind-Solar | | Wind-Bio | | Solar-Bio | | Wind-Solar-Bio | | |
|---|---|---|---|---|---|---|---|---|---|---|---|---|---|
| | | | | | Wind | Solar | Wind | Bio | Solar | Bio | Wind | Solar | Bio |
| 19 | 0 | **4.4** | **2.5** | **6.88** | **3.3** | **3.78** | **2.2** | **2.5** | **1.68** | **2.5** | **1.1** | **1.9** | **2.5** |
| 23 | 0 | 0 | 0 | 0 | 0 | 0 | 0 | 0 | 0 | 0 | 0 | 0 | 0 |
| 24 | 0 | 0 | 0 | **1** | 0 | **0.5** | 0 | 0 | 0 | 0 | 0 | 0 | 0 |
| 26 | 0 | 0 | 0 | 0 | 0 | 0 | 0 | 0 | 0 | 0 | 0 | 0 | 0 |
| 28 | 0 | **1.1** | **1** | **1.23** | **1.1** | **1.01** | 0 | **0. 5** | **1.12** | **0.5** | 0 | **0.7** | **0.5** |
| 32 | 0 | 0 | 0 | 0 | 0 | 0 | 0 | 0 | 0 | 0 | 0 | 0 | 0 |
| 33 | 0 | 0 | 0 | 0 | 0 | 0 | 0 | 0 | 0 | 0 | 0 | 0 | 0 |
| 35 | 0 | 0 | 0 | 0 | 0 | 0 | 0 | 0 | 0 | 0 | 0 | 0 | 0 |
| 37 | 0 | 0 | 0 | 0 | 0 | 0 | 0 | 0 | 0 | 0 | 0 | 0 | 0 |
| 38 | 0 | 0 | 0 | 0 | 0 | 0 | 0 | 0 | 0 | 0 | 0 | 0 | 0 |
| 39 | 0 | 0 | 0 | 0 | 0 | 0 | 0 | 0 | 0 | 0 | 0 | 0 | 0 |
| 40 | 0 | **2.2** | **1.5** | **3.17** | **1.1** | **2.16** | **1.1** | **1.5** | **1** | **1** | **1.1** | **0.99** | **1** |
| **Annual Energy Loss (MWh)** | **1676.23** | **1033.94 6** | **677.775** | **1105.25** | **906.7445** | | **701.984** | | **653.0435** | | **646.4955** | | |
| **Contribution of Each Renewable DG (MW)** | **0** | **7.7** | **5** | **12.28** | **5.5** | **7.45** | **3.3** | **4.5** | **3.8** | **4** | **2.2** | **3.78** | **4** |
| **DG Type as a % of the Total DG Installation** | **0** | **100%** | **100%** | **100%** | **42.2%** | **57.5%** | **42.3%** | **57.7%** | **48.7%** | **51.3%** | **22.5%** | **36.8%** | **40.7%** |

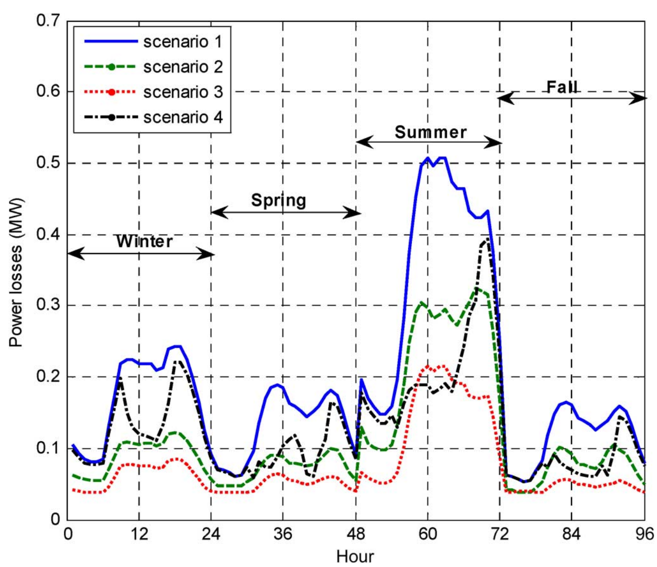


Fig. 5. Power losses during the first four scenarios.

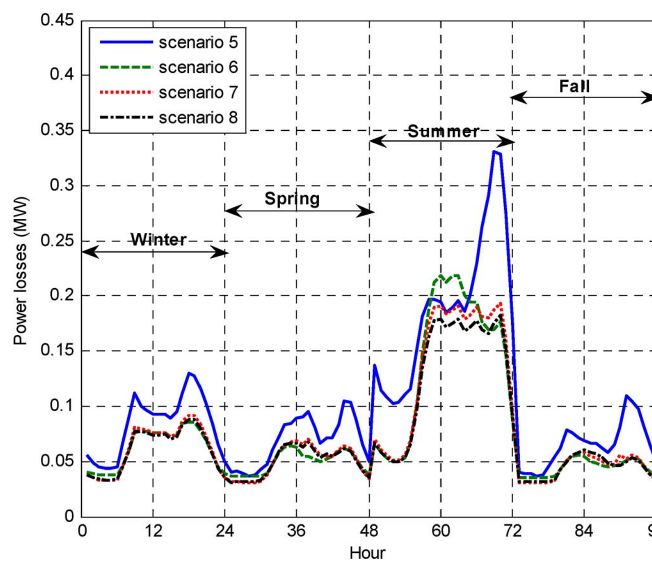


Fig. 6. Power losses during the last four scenarios.

in Table I. As shown in Fig. 3, it is obvious that, of all the turbines available, turbine 2 has the highest CF (0.2209); therefore, wind turbine type 2 is used for this study.

## *C. Solar Irradiance and PV Module Data*

The hourly solar irradiance data for the site under study have been utilized to generate a Beta pdf for each time segment and thus to calculate the CF for each available PV module, as listed in Table II. As shown in Fig. 4, it is obvious that, of all the modules available, module D has the highest CF (0.174); therefore, module type D is used for this study.

## *D. Biomass DG Unit Data*

For this study, the ratings available for the biomass DG units have been selected to be 1 MW and 0.5 MW.

## *E. Load Data*

From the hourly load data for the system under study and the IEEE-RTS system, the load profile is shown in Table III as a percentage of the annual peak load.

# X. RESULTS

The data for the seven main scenarios discussed in Section VIII are analyzed by the model to determine the optimal fuel mix of renewable DG units that will minimize system energy losses. The outcomes of the planning problem for the seven scenarios proposed and for the reference scenario are shown in Table IV and Figs. 5 and 6. The results reveal that regardless of the combination of the renewable resources used to calculate the optimal fuel mix, there is a significant reduction in the annual energy losses for all proposed scenarios when compared to the reference scenario. In addition, the same scenarios were repeated after relaxing the discrete size

TABLE V
RESULTS WITH DISCRETE DG SIZE CONSTRAINT RELAXED

| Candidate Buses | No DG | Wind | Biomass | Solar | Wind-Solar | | Wind-Bio | | Solar-Bio | | Wind-Solar-Bio | | |
|---|---|---|---|---|---|---|---|---|---|---|---|---|---|
| | | | | | Wind | Solar | Wind | Bio | Solar | Bio | Wind | Solar | Bio |
| 19 | 0 | **4.31** | **2.91** | **6.88** | **3.13** | **3.78** | **1.5** | **2.65** | **1.68** | **2.43** | **1.15** | **2.09** | **2.64** |
| 23 | 0 | 0 | 0 | 0 | 0 | 0 | 0 | 0 | 0 | 0 | 0 | 0 | 0 |
| 24 | 0 | 0 | 0 | **1** | 0 | **0.5** | 0 | 0 | 0 | 0 | 0 | 0 | 0 |
| 26 | 0 | 0 | 0 | 0 | 0 | 0 | 0 | 0 | 0 | 0 | 0 | 0 | 0 |
| 28 | 0 | **1.38** | **1** | **1.23** | **1** | **1.01** | 0 | **0.45** | **1.12** | **0.61** | 0 | **0.7** | **0.5** |
| 32 | 0 | 0 | 0 | 0 | 0 | 0 | 0 | 0 | 0 | 0 | 0 | 0 | 0 |
| 33 | 0 | 0 | 0 | 0 | 0 | 0 | 0 | 0 | 0 | 0 | 0 | 0 | 0 |
| 35 | 0 | 0 | 0 | 0 | 0 | 0 | 0 | 0 | 0 | 0 | 0 | 0 | 0 |
| 37 | 0 | 0 | 0 | 0 | 0 | 0 | 0 | 0 | 0 | 0 | 0 | 0 | 0 |
| 38 | 0 | 0 | 0 | 0 | 0 | 0 | 0 | 0 | 0 | 0 | 0 | 0 | 0 |
| 39 | 0 | 0 | 0 | 0 | 0 | 0 | 0 | 0 | 0 | 0 | 0 | 0 | 0 |
| 40 | 0 | **1.97** | **1.34** | **3.17** | **1.41** | **2.16** | **1.23** | **1.35** | **1** | **1.21** | **1** | **0.99** | **1.19** |
| Annual Energy Loss (MWh) | 1676.23 | 984.71 | 645.5 | 1105.25 | 873.09 | | 638.08 | | 631.47 | | 615.71 | | |
| Contribution of Each Renewable DG (MW) | 0 | 7.66 | 5.25 | 12.28 | 5.54 | 7.45 | 2.73 | 4.45 | 3.8 | 4.25 | 2.15 | 3.78 | 4.33 |
| DG Type as a % of the Total DG Installation | 0 | 100% | 100% | 100% | 42.6% | 57.4% | 38% | 62% | 47.2% | 52.8% | 21% | 37% | 42% |

TABLE VI
DIFFERENT COMBINATIONS OF LOAD AND WIND POWER (MATRIX $Cg$)

| State | Wind-based DG output as a percentage of rated power | Solar DG output as a percentage of rated power | Biomass DG output as a percentage of rated power | Loadas a percentage of peak load |
|---|---|---|---|---|
| 1 | 0 | 0 | 1 | 0.65 |
| 2 | 0 | 0.5 | 1 | 0.65 |
| 3 | 0 | 1 | 1 | 0.65 |
| 4 | 0.5 | 0 | 1 | 0.65 |
| 5 | 0.5 | 0.5 | 1 | 0.65 |
| 6 | 0.5 | 1 | 1 | 0.65 |
| 7 | 1 | 0 | 1 | 0.65 |
| 8 | 1 | 0.5 | 1 | 0.65 |
| 9 | 1 | 1 | 1 | 0.65 |

constraints in order to measure how far the outcomes of the MINLP are from the global optimal.

The results of this phase are presented in Table VI and analyzed below.

### A. Wind Versus Solar

Although solar irradiance and wind speed involve large amounts of uncertainty, the loss reduction that results in scenario 2 (only wind-based DG) is higher than for scenario 4 (only solar DG). An explanation is that for at least one-third of the year (at night), the output power of the solar DG units is almost zero, as shown in Figs. 7 and 8. During these periods, the system acts similarly to the way it does in scenario 1 (no DG connected to the system), which has a negative effect on the loss reduction achieved in this scenario.

### B. Biomass Impact on System Loss

The main advantage of the biomass DG is the firm output power generated, which is the basis for the following observations.

- The maximum reduction in loss occurs in scenario 8 (wind-solar-biomass).

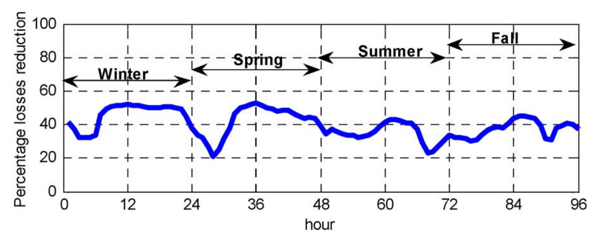


Fig. 7. Hourly percentage power loss reduction during scenario 2 (wind-based DG).

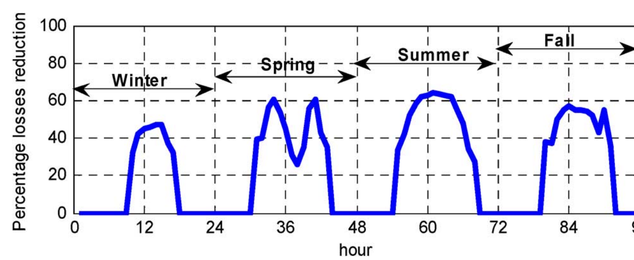


Fig. 8. Hourly percentage power loss reduction during scenario 3 (solar DG).

- All scenarios that include biomass DG are superior to other scenarios from a loss-reduction perspective, and biomass is the dominant renewable resource in these scenarios.
- The difference between the maximum penetration and the actual penetration (CF $\times$ rating of the DG) of the renewable DG units is reduced for the scenarios that include biomass resources, as shown in Fig. 9.

### C. Impact of the Discrete Size of the Renewable DG Units on the Annual Energy Loss

As expected, relaxing the discrete size constraints has a positive impact on the annual energy loss reduction, as shown in Tables IV and V. However, the improvement in the annual energy loss reduction is not more than 5% for any of the proposed scenarios, which means that the results obtained using the discrete size of the renewable DG units as one of the constraints are not far from the global optimality.

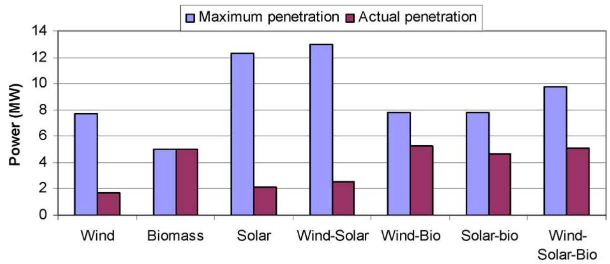


Fig. 9. Comparison of the maximum penetration and actual penetration for all scenarios.

TABLE VII
PROBABILITY OF DIFFERENT COMBINATIONS OF LOAD AND RENEWABLE OUTPUT POWER $[P(Cg)]$

| Stat | Probability | Stat | Probability | State | Probability |
|---|---|---|---|---|---|
| 1 | 0.3*0.4=0.12 | 4 | 0.6*0.4=0.24 | 7 | 0.1*0.4=0.04 |
| 2 | 0.3*0.5=0.15 | 5 | 0.6*0.5=0.30 | 8 | 0.1*0.5=0.05 |
| 3 | 0.3*0.1=0.03 | 6 | 0.6*0.1=0.06 | 9 | 0.1*0.1=0.01 |

The contribution of the proposed planning technique can be summarized as follows.

1) The proposed technique guarantees no violation of any of the system constraints under any operating conditions.
2) The technique guarantees the optimum allocation of the renewable DG units for all possible operating conditions.
3) A byproduct of the proposed technique is a power flow solution for all possible operating conditions, which will provide a useful database for the system operator.
4) Because the mathematical formulation is generic, the objective function can be expanded to accommodate additional terms, such as capital and running costs of the DG units, and therefore, this technique has applications beyond the minimization of energy loss.

## XI. CONCLUSION

In this paper, a probabilistic planning technique is proposed for optimally allocating different types of DG (i.e., wind-based DG, solar DG, and biomass DG) into the distribution system so as to minimize annual energy losses. Specifically, this technique is based on generating a probabilistic generation-load model that includes all possible operating conditions; hence, this model can be accommodated into a deterministic OPF formulation. The random behaviors of solar irradiance and wind speed are modeled by means of Beta and Rayliegh distributions, respectively. Biomass DG is considered as firm generation DG, and the load is modeled using the IEEE-RTS system. The optimization problem is formulated as MINLP, under a GAMS environment, taking into consideration the system's technical constraints, such as the voltage limits, the thermal limits of the feeder, the maximum investment capacity on each bus, the discrete size of the DG, and the maximum penetration limit of the DG units. The proposed planning technique has been applied to different scenarios for a typical rural distribution system provided by a local utility company. The results reveal that regardless of the combination of the renewable resources used to calculate the optimal fuel mix, there is a significant reduction in the annual energy loss for all scenarios proposed. Also for all scenarios, the proposed technique guarantees the optimal fuel mix for loss minimization during the entire planning period and ensures that, for all possible operating conditions, no system constraints will be violated.

## APPENDIX

Consider that for tth time segment (hour), the probability distribution for wind speed and solar irradiance are $\mathrm{W^t}$ and $\mathrm{S^t}$, respectively, and are given by $\mathrm{W^t} = [\{0, 0.3\}, \{0.5, 0.6\}, \{1, 0.1\}]$; $\mathrm{S^t} = [\{0, 0.4\}, \{0.5, 0.5\}, \{1, 0.1\}]$.

The first element of each set is the output of the DG as a percentage of the rated power; the second element is the probability of occurrence during the tth time segment. The load during this hour is assumed to be 0.65 of the peak load, while the biomass DG output is constant at the rated power.

The number of wind speed states $w = 3$.

The number of solar irradiance states $y = 3$.

The total number of states $N = 3 * 3 = 9$. Matrix $C_g$ is as shown in Table VI, while $P(C_g)$ is as shown in Table VII.

## REFERENCES

[1] J. O. Kim, S. K. Park, K. W. Park, and C. Singh, "Dispersed generation planning using improved Hereford Ranch algorithm," *Elect. Power Syst. Res.*, vol. 47, no. 1, pp. 47–55, Oct. 1998.
[2] M. Gandomkar, M. Vakilini, and M. Ehsan, "Optimal distributed generation allocation in distribution network using Hereford Ranch algorithm," in *Proc. Int. Conf. Electrical Machines and Systems*, Sep. 2005, vol. 2.
[3] T. Griffin, K. Tomsovic, D. Secrest, and A. Law, "Placement of dispersed generations system for reduced losses," in *Proc. 33rd Hawaii Int. Conf. System Science*, Maui, Hi, Jan. 2000.
[4] K. Nara, Y. Hayashi, K. Ikeda, and T. Ashizawa, "Application of Tabu search to optimum placement of distributed generations," in *Proc. IEEE PES Winter Meeting*, Jan. 2001, vol. 2.
[5] J. A. Greatbanks, D. H. Popovic, M. Begovic, A. Pregelj, and T. C. Green, "On optimization for security and reliability of power systems with distributed generation," in *Proc. IEEE Bologna Power Tech Conf.*, Bologna, Italy, Jun. 2003.
[6] D. H. Popovic, J. A. Greatbanks, M. Begovic, and A. Pregelj, "Placement of distributed generations and reclosers for distribution network security and reliability," *Int. J. Elect. Power Energy Syst.*, vol. 27, no. 5–6, pp. 398–408, Jun. 2005.
[7] P. N. Vovos, G. P. Harrison, A. R. Wallace, and J. W. Bialek, "Optimal power flow as a tool for fault level-constrained network capacity analysis," *IEEE Trans. Power Syst.*, vol. 20, no. 2, pp. 734–741, May 2005.
[8] V. H. M. Quezada, J. R. Abbad, and T. G. San Román, "Assessment of energy distribution losses for increasing penetration of distributed generation," *IEEE Trans. Power Syst.*, vol. 21, no. 2, pp. 533–540, May 2006.
[9] W. El-Khattam, K. Bhattacharya, Y. Hegazy, and M. M. A. Salama, "Optimal investment planning for distributed generation in a competitive electricity market," *IEEE Trans. Power Syst.*, vol. 19, no. 3, pp. 1674–1684, Aug. 2004.
[10] G. Celli, E. Ghiani, S. Mocci, and F. Pilo, "A multiobjective evolutionary algorithm for the sizing and siting of distributed generation," *IEEE Trans. Power Syst.*, vol. 20, no. 2, pp. 750–757, May 2005.
[11] C. Wang and M. H. Nahrir, "Analytical approaches for optimal placement of distributed generation sources in power systems," *IEEE Trans. Power Syst.*, vol. 19, no. 4, pp. 2068–2076, Nov. 2004.
[12] G. Celli and F. Pilo, "Optimal distributed generation allocation in MV network," in *Proc. 22nd IEEE PES Int. Conf. Power Industry and Computer Applications*, Sydney, Australia, May 2001.
[13] G. Celli and F. Pilo, "MV network planning under uncertainty on distributed generation penetration," in *Proc. IEEE PES Summer Meeting*, Jul. 2001, vol. 1.

[14] G. Carpinelli, G. Celli, F. Pilo, and A. Russo, "Distributed generation sitting and sizing under uncertainty," in *Proc. IEEE Porto Power Tech Conf.*, Porto, Portugal, Sep. 2001.
[15] L. F. Ochoa, C. J. Dent, and G. P. Harrison, "Maximisation of intermittent distributed generation in active networks," in *Proc. CIRED Seminar 2008: SmartGrids for Distribution*, Frankfurt, Germany, Jun. 23–24, 2008.
[16] A. Keane and M. O'Malley, "Optimal distributed generation plant mix with novel loss adjustment factors," in *Proc. IEEE PES General Meeting*, Jun. 2006.
[17] A. Keane and M. O'Malley, " Optimal utilization of distribution networks for energy harvesting," *IEEE Trans. Power Syst.*, vol. 22, no. 1, pp. 467–475, Feb. 2007.
[18] [Online]. Available: http://www.powerauthority.on.ca/sop/.
[19] *IEEE Standard for Interconnecting Distributed Resources With Electric Power Systems*.
[20] R. Karki and R. Billinton, "Cost-effective wind energy utilization for reliable power supply," *IEEE Trans. Energy Convers.*, vol. 19, no. 2, pp. 435–440, Jun. 2004.
[21] Z. M. Salameh, B. S. Borowy, and A. R. A. Amin, "Photovoltaic module-site matching based on the capacity factors," *IEEE Trans. Energy Convers.*, vol. 10, no. 2, pp. 326–332, Jun. 1995.
[22] G. Boyle, *Renewable Energy*. Oxford, U.K.: Oxford Univ. Press, 2004.
[23] J. M. S. Pinheiro, C. R. R. Dornellas, and A. C. G. Melo, "Probing the new IEEE reliability test system (RTS-96): HL-II assessment," *IEEE Trans. Power Syst.*, vol. 13, no. 1, pp. 171–176, Feb. 1998.
[24] J. Hetzer, C. Yu, and K. Bhattarai, "An economic dispatch model incorporating wind power," *IEEE Trans. Energy Convers.*, vol. 23, no. 2, pp. 603–611, Jun. 2008.
[25] *"GAMS-A User's Guide,"* 2008, New York.

**Y. M. Atwa** (S'06) was born in Alexandria, Egypt, in 1975. He received the B.Sc. and M.Sc. degrees in electrical engineering from Alexandria University, Alexandria, Egypt, in 1998 and 2004, respectively. He is currently pursuing the Ph.D. degree in the Department of Electrical and Computer Engineering, University of Waterloo, Waterloo, ON, Canada.

His research interests are distribution system planning, power quality, reliability, and distributed generation.

**E. F. El-Saadany** (SM'05) was born in Cairo, Egypt, in 1964. He received the B.Sc. and M.Sc. degrees in electrical engineering from Ain Shams University, Cairo, Egypt, in 1986 and 1990, respectively, and the Ph.D. degree in electrical engineering from the University of Waterloo, Waterloo, ON, Canada, in 1998.

Currently, he is an Associate Professor in the Department of Electrical and Computer Engineering, University of Waterloo. His research interests are distribution system control and operation, power quality, distributed generation, power electronics, digital signal processing applications to power systems, and mechatronics.

**M. M. A. Salama** (F'02) received the B.Sc. and M.Sc. degrees in electrical engineering from Cairo University, Cairo, Egypt, in 1971 and 1973, respectively, and the Ph.D. degree in electrical engineering from the University of Waterloo, Waterloo, ON, Canada, in 1977.

Currently, he is a Professor in the Department of Electrical and Computer Engineering, University of Waterloo. His interests include the operation and control of distribution systems, power-quality monitoring and mitigation, asset management, and electromagnetic. He has consulted widely with government agencies and the electrical industry.

Dr. Salama is a registered Professional Engineer in the Province of Ontario.

**R. Seethapathy** (M'76) is currently Manager—Distributed Generation, and Advanced Grid Development, Hydro One Networks, Inc., Toronto, ON, Canada.

Mr. Seethapathy sits on several T&D/DG committees at the PES/IEEE and CIGRE. He is also a Registered Professional Engineer in the Province of Ontario.